applied sciences

Article

Study on Flow Characteristics of Venturi Accelerated Vortex Drainage Tool in Horizontal Gas Well

Hongtao Zhang [1,2,3], Yan Xu [1,*], Meng Cai [2,3], Junliang Li [2,3], Mingxi Feng [2,3] and Xiaochuan Zhang [2,3]

1 College of Mechanical Science and Engineering, Northeast Petroleum University, Daqing 163318, China; hongtao996@163.com
2 Daqing Oil Field Production Technology Institute, Daqing 163000, China; cyycaimeng@petrochina.com.cn (M.C.); bullsliang1982@163.com (J.L.); fengmingxi2012@163.com (M.F.); cyyzxc1@163.com (X.Z.)
3 Heilongjiang Provincial Key Laboratory of Oil and Gas Reservior Stimulation, Daqing 163000, China
* Correspondence: xuyanzhf@nepu.edu.cn

Abstract: Vortex drainage gas recovery has been used to carry liquid from gas wells. However, the traditional vortex tools in gas wells cannot produce long effective distance spiral flow at a low gas flow rate, and their operating mechanism has not been thoroughly analyzed. In this paper, the venturi acceleration vortex tool for a horizontal gas well is designed to improve drainage performance. The tube drainage, the vortex tool, and the venturi accelerated vortex tool were applied in a horizontal tube to investigate their drainage capacities by a horizontal well multiphase flow experimental device. The influence of different gas flow rates and liquid flow rates on the length of the spiral flow and pressure drop produced by the three tools was analyzed. The results show that the vortex tool can convert the gas–liquid mixing flow into the gas–liquid separation flow, that is, the liquid flows spirally along the wall and the gas flows in the center of the horizontal tube. Compared with the vortex tool, the venturi accelerated vortex tool can form a longer and more stable spiral flow. The laminar spiral flow reduces the total pressure drop in the tube. The length of the spiral flow increases with the increase in the gas flow rate. With the increase in the liquid flow rate, the spiral flow is not clear because of the turbulent flow. The length of the spiral flow and the pressure drop for the venturi accelerated vortex tool with different gas and liquid flow rates are analyzed to guide the application of the tool. This study provides a new means for the drainage of a horizontal gas well and further clarifies the working mechanism of the vortex drainage tool.

Keywords: horizontal wells; drainage gas recovery; venturi; vortex tool

MSC: 76T10; 76-05

Citation: Zhang, H.; Xu, Y.; Cai, M.; Li, J.; Feng, M.; Zhang, X. Study on Flow Characteristics of Venturi Accelerated Vortex Drainage Tool in Horizontal Gas Well. *Appl. Sci.* **2024**, *14*, 2944. https://doi.org/10.3390/app14072944

Academic Editor: Jianzhong Lin

Received: 9 February 2024
Revised: 6 March 2024
Accepted: 13 March 2024
Published: 31 March 2024

1. Introduction

The application of horizontal wells can achieve a high level of production with fewer wells; these have become the main exploitation method used in deep natural gas fields. However, the liquid accumulation in the wellbore of horizontal wells leads to a decrease in gas production, which is a key issue faced by various large gas fields. In view of horizontal well drainage gas recovery, numerous scholars have carried out relevant research. The vortex tool has been used more and more for drainage gas recovery based on the swirling flow mechanism.

When the vortex tool is used, a gas–liquid two-phase fluid flow occurs through it to generate tangential velocity and form the swirling flow. Due to the centrifugal force, the liquid phase with a higher density flows along the wall, and the gas phase with a lower density flows in the center of the tube, which improves the effect of the drainage. Many scholars have studied the working mechanism of vortex tools and verified their effectiveness. Wang et al. [1] analyzed the drainage of gas wells. The radial distribution of the liquid phase and the gas–liquid flow pattern have been investigated at the wellhead. The influence of the gas and liquid production capacity of gas wells and the main geometric parameters of vortex tools on the flow field were obtained. In order to evaluate the drainage effect of the internal vortex tool, Guo et al. [2] simulated the flow field and the liquid-carrying process of the gas–liquid two-phase fluid in the wellbore before and after the internal vortex tool was attached to the bottom of the tubing. The experimental results show that the internal vortex tool can effectively improve the liquid-carrying capacity and the flow pattern of the wellbore fluid and reduce the pressure drop. At the same time, the gas–liquid two-phase flow pattern and the pressure drop under different flow parameters were studied by numerical simulation. Finally, the experimental results were compared with the numerical simulation results, and it was found that the error of the pressure drop is within 10%. Gou et al. [3] carried out a numerical simulation of three internal swirling tools and analyzed the drainage recovery efficiency and the vortex characteristics of the swirling flow field downstream of the tools. By the energy efficiency analysis of the three structures, it was found that the three-leaf spiral tube is more suitable to apply during the initial stage of drainage, while the internal vortex tube is more conducive during the stable stage of drainage. The feasibility of the internal swirling tool in horizontal gas wells is demonstrated. Cai et al. [4] analyzed the physical process of eddy current tools for the drainage gas recovery, established a numerical simulation model, and developed the optimized design software. According to the eddy flow mechanism, the geometric parameters of eddy current tools, which are more suitable for gas well reservoirs, were determined, and the positioning depth of the vortex tool was calculated according to the Bernoulli equation. The field test results show that the application of eddy current tools resulted in effective gas–liquid separation, which is beneficial to increase the production of natural gas. Wu [5,6] analyzed the forces of liquid droplets in the swirling flow field of wellbores on the basis of two-phase fluid dynamics theories, establishing the motion equations of fluid droplets along axial and radical directions. The formula for calculating the optimal helical angle of vortex tools was established. Zhang [7] established a mechanistic model for the prediction of the swirling annular two-phase flow behavior downstream of the vortex tool, which has a guiding significance for the optimization design and field application of vortex tools.

The structural parameters of vortex tools are crucial for their drainage and gas extraction effectiveness. Wu et al. [5], based on two-phase flow theory, analyzed the forces acting on droplets in the rotating flow field of the wellbore. They established equations for the axial and radial movement of droplets and the calculation formula for the optimal helix angle of the vortex tool, validating the reliability of the optimal helix angle calculation formula. Zhou et al. [8] conducted two-phase vortex flow experiments in the wellbore, studying the impact of the structural parameters of the vortex tool on drainage effectiveness. The results indicated that enhancing the sealing on both sides of the flow channel and reducing the flow channel size can improve the effectiveness of the vortex tool. Ren et al. [9] established models for the gas–liquid separation efficiency and the pressure loss of the vortex tool, studying the impact of structural parameters on the liquid-carrying performance and the pressure loss of the vortex tool. They improved the vortex tool based on the research results. The field test results showed that the optimized vortex tool is beneficial for increasing gas well production. Guo et al. [10], by numerical simulation and theoretical calculation, studied the separation efficiency of two-phase flow in a double-helix separator. The results showed that the separation efficiency of the helical separator increased with the increase in the gas–liquid ratio and overall gas–liquid flow rate. Under certain conditions of helix number and gas–liquid ratio, there exists an optimal pitch. Zhang et al. [11] used an orthogonal experimental method to systematically study the attenuation characteristics, effective swirl length, and various other factors affecting the decay of vertical pipe swirl. The authors obtained the relationship between the initial swirl intensity and the decay rate of swirl intensity, proposed a comprehensive decay model for the swirl intensity, and established an evaluation method of the effective vortex length. The goal was to determine the optimal structure of the vortex tool in typical gas wells. In another interesting work, Huang et al. [12] designed a vortex tool and conducted computational fluid dynamics analysis of its drainage and gas extraction efficiency in horizontal wells to optimize its structure. The results indicated that the vortex tool can increase the gas phase velocity and achieve gas–liquid separation. Zhang et al. [13] attempted to reveal the regularity of the critical gas velocity in the swirl field generated by the vortex tool. The authors established a model for calculating the critical gas velocity in vortex drainage wells. The analysis included the impact of the helix angle and the vortex tool hub diameter on the magnitude of the reduction in critical gas velocity. The experimental validation demonstrated that the model can predict the critical gas velocity under different production conditions with different vortex tools. The critical gas velocity increases with the increase in the helix angle and decreases with the increase in the hub diameter. Zhang et al. [14] conducted experiments to study the gas–liquid flow pattern and pressure drop when the vortex tool was inserted into the tube with accumulated liquid at the well bottom and compared it with a regular tube. The impacts of the structural parameters and the stages of the vortex tool on pressure drop were examined. From the acquired experimental results, it was indicated that the insertion of the vortex tool is advantageous for an earlier transition to the circumferential flow, and the induced vortex can suppress liquid fallback. The helix angle of the spiral guide plate has a more significant effect on the pressure drop than its length. By changing the helix angle, the total pressure drop and downstream pressure gradient are significantly reduced, even below that of a regular tube. CFD numerical simulations have also been deployed to study the gas–liquid two-phase flow and highlight the impact of production parameters and tool structures on the performance of vortex drainage [15–17]. The underlying mechanism of the vortex downhole tool to improve production efficiency and the geometric parameter optimization method have been numerically investigated, suggesting that the vortex downhole tool can reduce the flow pressure drop [18].

New eddy current tools that are different from traditional structures have also been designed [19]. Liang et al. [20], for large pressure loss and short effective distance of traditional vortex tools in gas wells, designed and installed the organic combination of jet vortex drainage and gas production tools. The gas–liquid mixture before and after the jet vortex tool was analyzed, and the flow trajectory, the pressure loss, and the liquid volume fraction change were investigated. The comprehensive influence of each structural parameter on the effective working distance was optimized, and the optimal structural parameters of the jet vortex tool were obtained. The results showed that the critical liquid-carrying flow rate and pressure loss were reduced by using the jet vortex tool, whereas the axial velocity, initial velocity of gas phase and liquid phase, and the effective flow distance increased. As a result, the liquid-carrying capacity of gas wells was significantly improved. Liang et al. [21] proposed a new type of vortex drainage solution that combined self-excited oscillating pulsed jet and swirling flow. On the basis of theoretical analysis and experimental research, the numerical simulation results were compared with the drainage performance of conventional swirling tools. The results indicated that the new swirl tool can improve the liquid-carrying capacity of gas wells by changing the flow pattern of the gas–liquid medium without increasing energy consumption. Based on the Coanda effect, Shi et al. [22] established a numerical model of the double-vortex anti-friction tool. At the same time, the authors studied the influence of different geometric parameters on the vibration characteristics of the double-vortex anti-friction tool. The results showed that the double-vortex anti-friction tool can produce larger pressure drop and vibration frequency, and the pressure drop change process is more stable and has a better anti-friction effect. The change in the geometric parameters of the double-vortex anti-friction tool not only affects the pressure drop and the oscillation frequency but also the pressure drop.

In summary, many vortex tools for drainage in gas wells have been developed in the literature. However, the combination of the venturi acceleration tools and vortex tools for drainage and gas recovery has been scarcely examined. In particular, a deep understanding of the evaluation and analysis of swirl length is required. To effectively address this issue, in this work, the venturi accelerated vortex tool of the horizontal gas well was designed and the multiphase flow experimental device of the horizontal well was set up. The horizontal well drainage and gas recovery experiments for the tube drainage, the vortex tool, and the venturi accelerated vortex tool were carried out. Additionally, the drainage effect of the venturi accelerated vortex tool was evaluated. The impact of the different gas and liquid flow rates on swirl length and pressure drop were thoroughly analyzed. The mechanism of venturi accelerated vortex tool drainage was determined, which can provide guidance for the future applications of vortex tools.

2. Structure and Working Principle of Venturi Accelerated Vortex Tool

To enhance the liquid-carrying capacity of the horizontal wellbore, discharge liquid load, and increase gas well production, a venturi accelerated vortex tool for horizontal gas wells was developed and designed, as shown in Figure 1. The specific structural parameters are detailed in Tables 1 and 2.

Figure 1. Venturi accelerated vortex tool physical map.

Table 1. Structure parameters of vortex tool.

Length (mm)	Outer Diameter (mm)	Number of Helixes	Helix Length (mm)	Helix Width (mm)	Helix Height (mm)
400	50	4	70	6	10

Table 2. Structure parameters of venturi acceleration structure.

Length (mm)	Outer Diameter (mm)	Inner Diameter (mm)	Throat Diameter (mm)	Contraction Angle (°)	Diffusion Angle (°)
550	50	40	20	22	8

The outer diameter of the venturi accelerated vortex tool is consistent with that of the coiled tubing. The four-helix swirl structure was designed in the tool. It was attached to the bottom of the coiled tubing in the horizontal section. The flow pattern of the gas and liquid mixture flow can be transformed to swirl laminar flow with gas inside and liquid outside in the horizontal section, as shown in Figure 2. This achieved gas–liquid separation flow can induce the flow of the gas along the center of the horizontal tube, while the liquid flows spirally along the wall due to the impact of the centrifugal force. Simultaneously, the inlet velocity of the vortex tool is increased, the distance of the swirling flow is extended, and the drainage efficiency is enhanced by the design of the venturi acceleration structure.

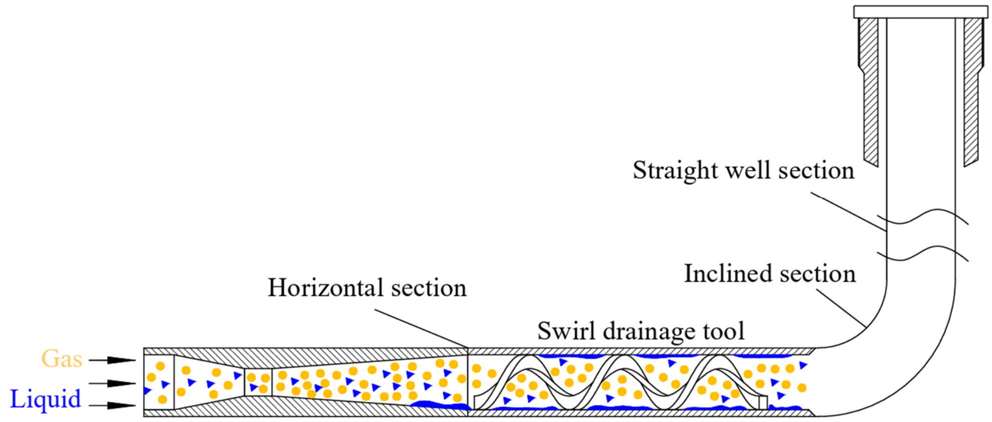

Figure 2. Working principle diagram of horizontal well swirl drainage.

3. Experimental Device and Method

The multiphase flow experimental apparatus was designed and set up to conduct experiments on the swirl drainage of natural gas in horizontal wells. The apparatus primarily consists of a liquid inlet system, an air inlet system, a simulated test tube system, a gas–liquid separation measurement system, and a data acquisition control system, as depicted in Figure 3. The physical photograph of the multiphase flow experimental apparatus is shown in Figure 4. The automatic control system of the device was used to control the opening and closing of the electric valves in the tube, as well as regulate the gas–liquid flow rates. The high-precision pressure gauges and flow meters were also installed along the tube to collect the pressure and the flow rate. The data acquisition and storage system was set to record the data every 5 s.

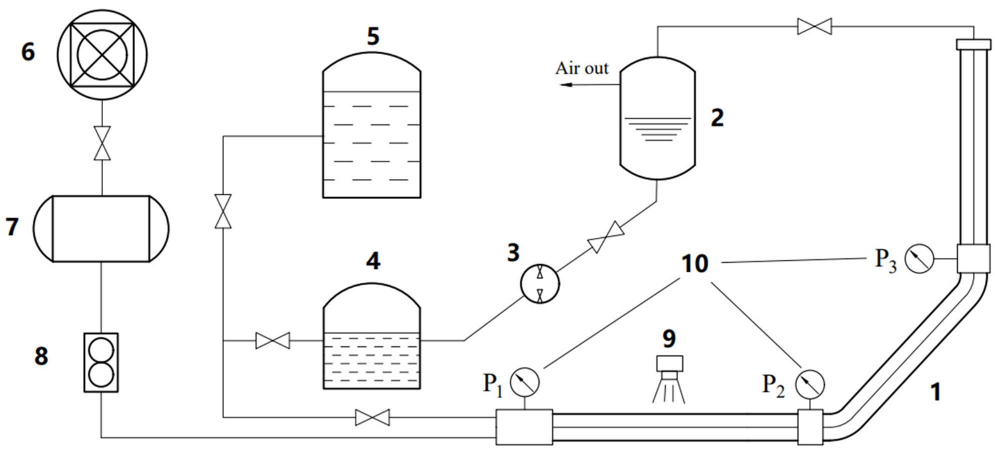

Figure 3. Multiphase flow experiment device composition diagram. 1 simulated horizontal well; 2 gas–liquid separator; 3 liquid pump; 4 waste liquid pool; 5 sample storage tank; 6 gas compressor; 7 gas storage tank; 8 gas flowmeter; 9 camera system; 10 pressure-measuring device.

Utilizing the established experimental apparatus, liquid-carrying performance experiments were conducted in the absence of a vortex tool (tube drainage), with the vortex tool, and with the venturi accelerated vortex tool. The main bodies of the tools were made using transparent Perspex for easily observing the changes in the flow patterns of the gas–liquid two-phase flow. For the venturi accelerated vortex tool, the vortex tool was connected to the venturi accelerator by the flanges. The gas and liquid mixture flows first through the venturi accelerator, then through the vortex tool, out of the tool, and finally enters the horizontal section. During the testing process, pressure tests were performed at the inlet (before the vortex tool), the outlet of the horizontal tube, and the outlet of the vertical tube. Simultaneously, the flow patterns of the gas–liquid mixture in the horizontal tube were photographed, and the lengths of spiral flow were observed. Liquid-carrying experiments with different parameters were also performed by adjusting the power of the liquid pump and the gas compressor, as well as the opening of the valve, to change the liquid and gas flow rates. Compressed air was used to simulate the natural gas and pure water was used to simulate the accumulated liquid. The specific experimental parameters are provided in Table 3.

Figure 4. Multiphase flow experiment device physical diagram.

Table 3. Experimental parameters of drainage in horizontal gas wells.

Experimental Conditions	Specific Parameters
Temperature (°C)	20–25
Liquid flow rate (L/min)	1, 3, 5, 10, 15
Gas flow rate (m^3/h)	100, 200, 300, 400, 500, 600
Liquid Reynolds number	420, 1260, 2101, 4202, 6303
Gas Reynolds number $\times 10^5$	0.51, 1.02, 1.53, 2.04, 2.55, 3.06

4. Results and Discussion

4.1. The Liquid-Carrying Capacity with Different Gas Flow Rates

The drainage experiments of the horizontal tube were carried out using the three kinds of tube drainage, the vortex tool, and the venturi accelerated vortex tool. To compare the drainage performance of the different tool structures, a liquid flow rate of 3 L/min and a gas flow rate ranging from 100 m^3/h to 600 m^3/h were used, and the acquired results were thoroughly investigated. The flow pattern of the horizontal tube was photographed as the gas–liquid mixture flowed through the different tools. The captured spiral flow patterns are displayed in Figure 5.

As shown in Figure 5, when the liquid flow rate is 3 L/min and the gas flow rate is 100 m^3/h, the gas–liquid mixture flows in a typical layered flow pattern using the tube drainage. It is interesting to notice that no obvious sprial flow is formed using the vortex tool, and the short sprial flow is formed at the tool's outlet using the venturi accelerated vortex tool. Additionally, the flow shows a trend of transitioning from layered flow to spiral flow downstream. When the gas flow rate is increased to 200 m^3/h, spiral flow also occurs with the vortex tool. The spiral flow is clearer for the venturi accelerated vortex tool, and the length of spiral flow is slightly longer. However, after flowing a certain distance the flow essentially returns to laminar flow. As the gas flow rate continues to increase, the length of the spiral flow significantly increases. It can be clearly observed that the spiral flow produced by the venturi accelerated vortex tool is significantly longer than that of the other tool. When the gas flow rate reaches 600 m^3/h, a stable spiral flow is formed. The spiral flow fills the horizontal observation tube (the length is 2 m) with the vortex and venturi accelerated vortex tool. Nevertheless, the flow is dispersed turbulent flow with the tube drainage. This effect indicates that the vortex tool can effectively separate gas and liquid, transforming the mixed gas–liquid turbulent flow into a laminar spiral flow. The measured length of the spiral flow is shown in Figure 6. As shown in this figure, the length of spiral flow formed by the venturi accelerated vortex tool is greater than that produced by the vortex tool alone. This is attributed to the presence of the constriction structure inside the venturi tube, which accelerates the fluid and promotes the formation of the spiral flow.

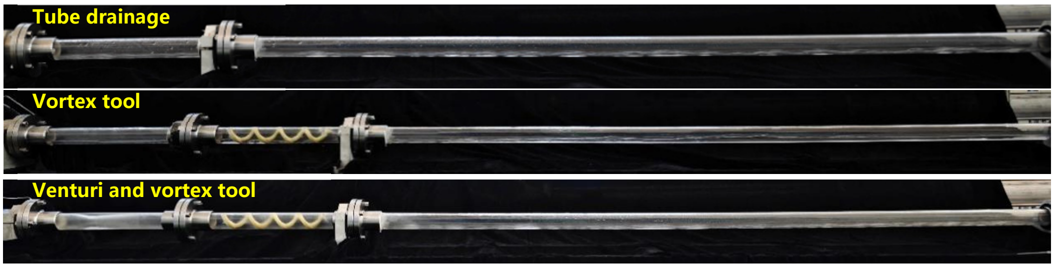

(**a**) 100 m³/h

(**b**) 200 m³/h

(**c**) 300 m³/h

(**d**) 400 m³/h

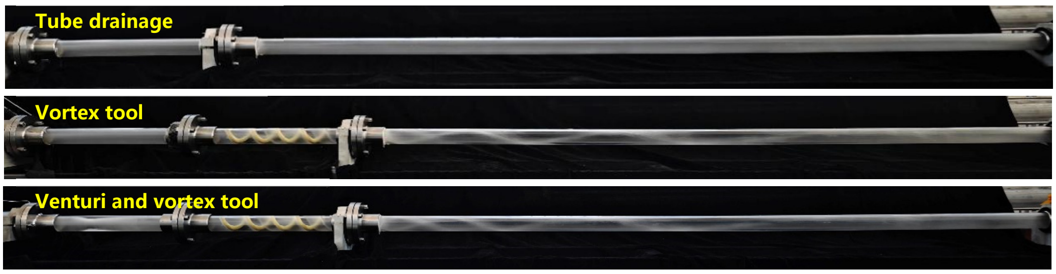

(**e**) 500 m³/h

Figure 5. *Cont.*

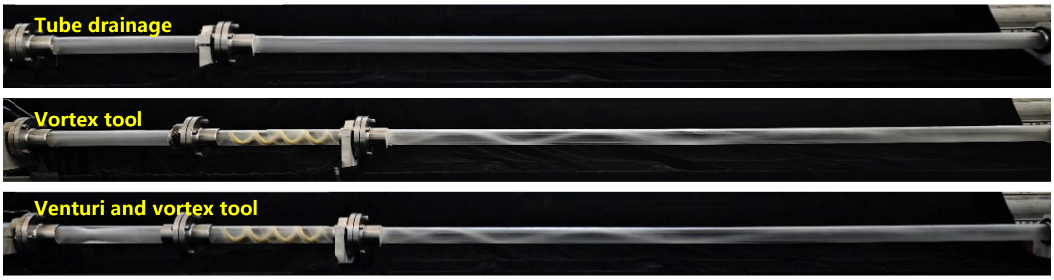

(**f**) 600 m³/h

Figure 5. Spiral flow patterns with liquid flow rate of 3 L/min and gas flow rates of 100 to 600 m^3/h using different tools.

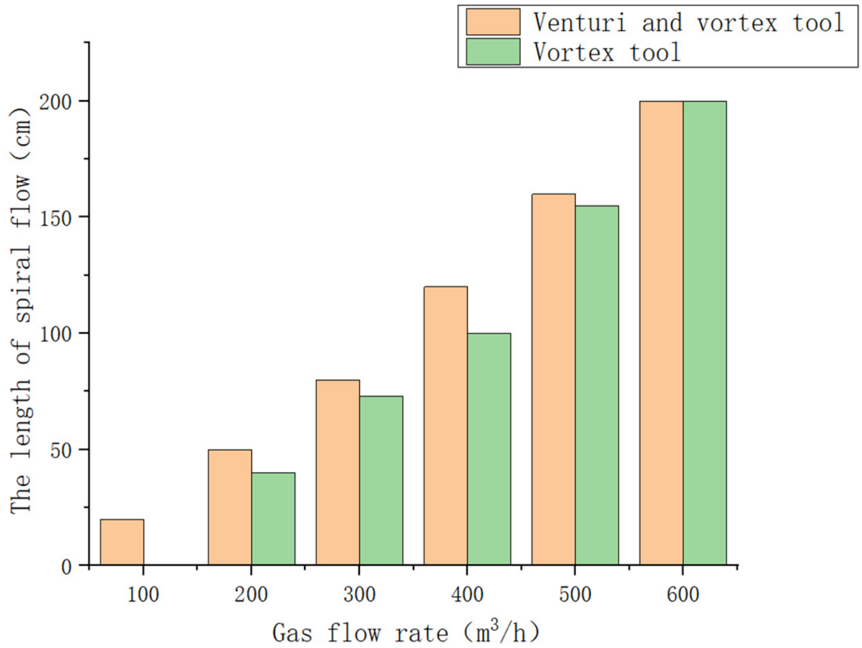

Figure 6. The length of spiral flow with liquid flow rate of 3 L/min and gas flow rates of 100 to 600 m^3/h.

To further analyze the flow patterns of spiral flow for the venturi accelerated vortex tool, the spiral flow pattern with different gas flow rates was analyzed. The photographed flow fluid is shown in Figure 7 when the inlet liquid flow rate is 3 L/min and the gas flow rate varies from 100 m^3/h to 600 m^3/h. As the gas flow rate increases, the length of the spiral flow is also gradually increased, the pitch of the spiral flow is gradually reduced, and the spiral flow becomes more stable. When the gas flow rate reaches 500 m^3/h, with the increase in gas flow rate, the length and pitch of spiral flow remain basically unchanged. The stable spiral flow is conducive to the carrying of liquid. According to the literature, due to the guidance of the spiral, the fluid obtains centrifugal acceleration, and the heavier liquid is thrown to the pipe wall, forming a rotary flow. As a result, the compressible gas is expanded, and the gas velocity at the center of the wellbore is increased [23].

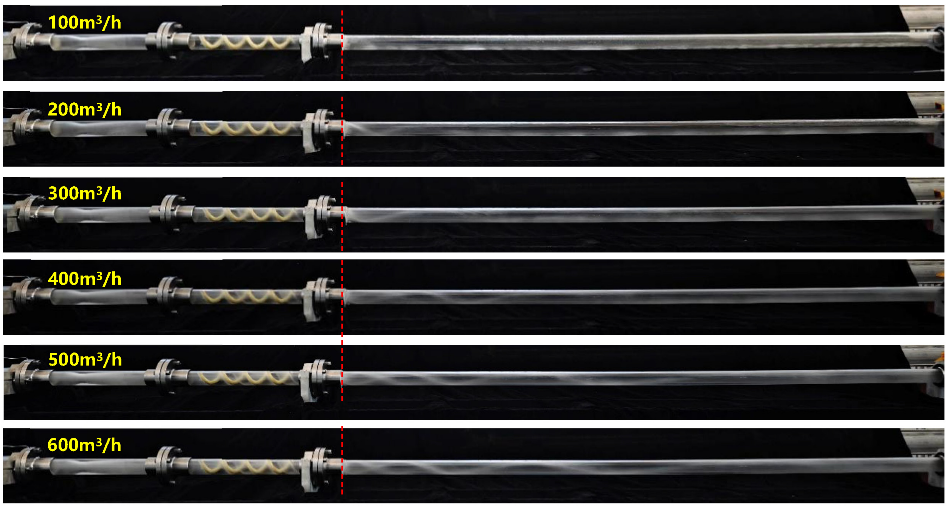

Figure 7. Spiral flow patterns for the venturi and vortex tool, with liquid flow rate of 3 L/min and gas flow rates of 100 m^3/h to 600 m^3/h.

4.2. Pressure Drop with Different Gas Flow Rates

When the liquid flow rate is 3 L/min and the gas flow rate is 100–600 m^3/h, the instantaneous pressure drop in the horizontal tube (P_1–P_2) was measured by conducting different experiments with the tube drainage, the vortex tool, and the venturi and vortex tool, as shown in Figure 8.

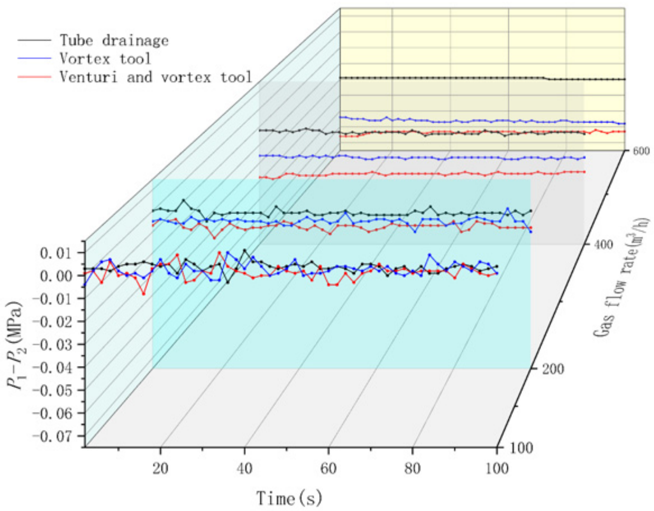

Figure 8. Instantaneous pressure drop of different tools in the horizontal tube with liquid flow rate of 3 L/min and gas flow rates of 100–600 m^3/h. (Supplementary Figure S1).

Analyzing the changes in instantaneous pressure drop in Figure 8, it is evident that as the gas flow rate increases, the vacuum level used by the venturi accelerated vortex tool is significantly higher, in striking contrast to using the vortex tool alone. Therefore, the venturi accelerated vortex tool induces the negative pressure drop to increase downstream in the horizontal tube, resulting in a more stable spiral flow. Hence, the length of the spiral flow is extended, and the liquid-carrying performance is effectively enhanced. The fluctuations of the pressure drop gradually decreased with the increase in the gas flow rate, and the instantaneous pressure drop became more stable.

According to the above-mentioned analysis, the pressure drop in the horizontal tube was averaged, as shown in Figure 9, and the total pressure drop in the horizontal and vertical tube (P_1–P_3) was averaged, as shown in Figure 10.

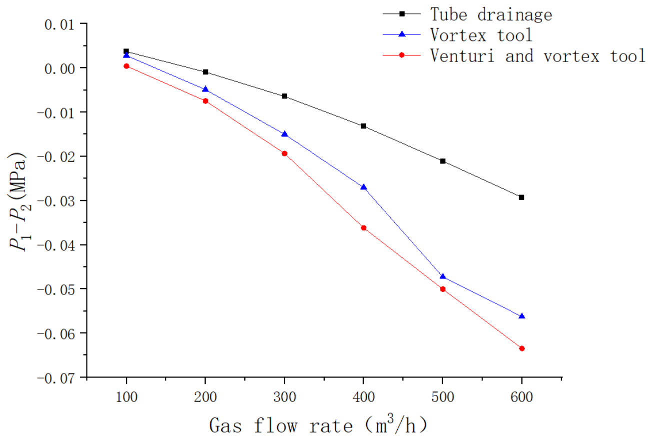

Figure 9. The average pressure drop of different tools in the horizontal tube with the liquid flow rate of 3 L/min and gas flow rates of 100–600 m^3/h.

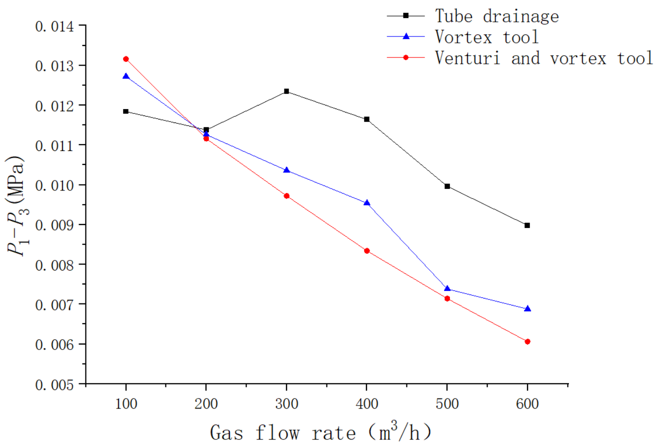

Figure 10. The average total pressure drop of different tools in the horizontal and vertical tube, with the liquid flow rate of 3 L/min and gas flow rates of 100–600 m^3/h.

Figure 9 illustrates that the average negative pressure drop generated by the venturi accelerated vortex tool is the highest among the three tools, followed by that of the vortex tool. On the contrary, the average negative pressure drop generated by the tube drainage is the lowest. As the gas flow rate increases, the average negative pressure drop is also increased. The increase in the negative pressure drop becomes more significant with the application of higher gas flow rates. This result indicates that the increase in gas flow rate is beneficial for drainage, and the venturi accelerated vortex tool can further improve the liquid-carrying performance.

Figure 10 explains the average total pressure drop in both the horizontal and vertical tubes. When the vortex tool was used, the total pressure drop increased at low gas flow rates (<200 m^3/h). The main reason is that under low gas flow conditions, the liquid for the tube drainage first forms a stable stratified flow, while the liquid for the vortex tool and the venturi accelerated vortex tool forms an unstable spiral laminar flow. The unstable spiral laminar flow in the vortex tools increased the total pressure drop. As a result, the stably stratified flow in the tube drainage generated a lower pressure drop than that of the other two tools. However, when the gas flow rate reached 200 m^3/h, the total pressure drop decreased for the vortex tool, especially for the venturi accelerated vortex tool. This effect is consistent with Ren's conclusions suggesting that the pressure loss of the vortex tool gradually decreased as the gas flow rate increased [9]. This is due to the formation of a relatively stable spiral laminar flow for the vortex tool as the liquid flows along the wall and the gas flows along the center of the tube. This effect reduces the friction losses in the gas–liquid mixed flow, thereby reducing the overall pressure losses in the system.

Therefore, the venturi accelerated vortex tool results in smaller total pressure loss. When the gas flow rate increased to 300 m^3/h, the liquid in the tube drainage formed an unstable stratified flow, resulting in an increasing pressure drop. As the gas flow rate continued to increase, the annular flow and fog flow were gradually formed, which induced a reduction in the pressure drop for the tube drainage. However, these were still higher than for the other two vortex tools.

4.3. The Liquid-Carrying Capacity with Different Liquid Flow Rates

To further investigate the impact of different liquid flow rates on the drainage performance of the tools, liquid-carrying experiments with the gas flow rate of 300 m^3/h and the liquid flow rates of 1, 3, 5, 10, and 15 L/min were conducted. Photographs of the spiral flow patterns in the horizontal tube with three tools are depicted in Figure 11.

As shown in Figure 11, it can be observed that when the gas flow rate is 300 m^3/h and the liquid flow rate varies from 1 L/min to 5 L/min, the fluid pattern changes from laminar flow to unstable annular flow for the tube drainage. Moreover, the fluid flows according to spiral laminar flow for the vortex tools. The venturi accelerated vortex tool can make this flow more stable than the vortex alone. When the liquid flow rate reaches 10–15 L/min, the kinetic energy of the gas flow is not enough to drive the liquid for the tube drainage. At this point, the vortex tool has a critical role. Although the stable flow characterized by the coupling of the spiral and turbulent flows was formed for the vortex tool, the liquid can be carried relatively well to flow out of the horizontal tube.

To analyze the flow patterns of the spiral flow at different liquid flow rates, when the gas flow rate was 600 m^3/h, spiral flow experiments with different liquid flow rates of 1–15 L/min for the venturi accelerated vortex tool were conducted, as shown in Figure 12.

(**a**) 1 L/min

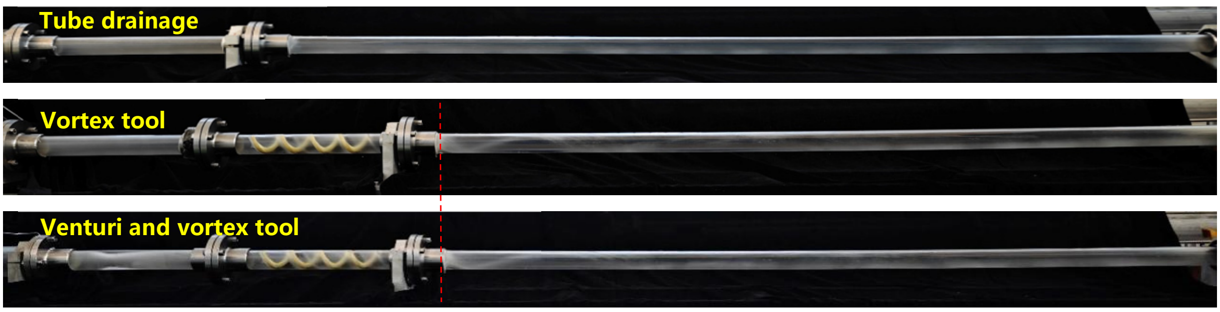

(**b**) 3 L/min

Figure 11. *Cont.*

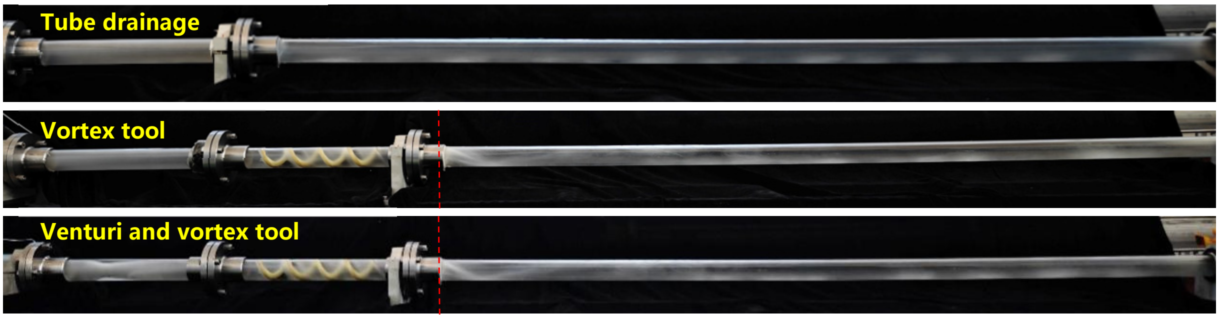

(**c**) 5 L/min

(**d**) 10 L/min

(**e**) 15 L/min

Figure 11. Spiral flow patterns of different tools with various liquid flow rates (1, 3, 5, 10, 15 L/min) and the gas flow rate of 300 m^3/h.

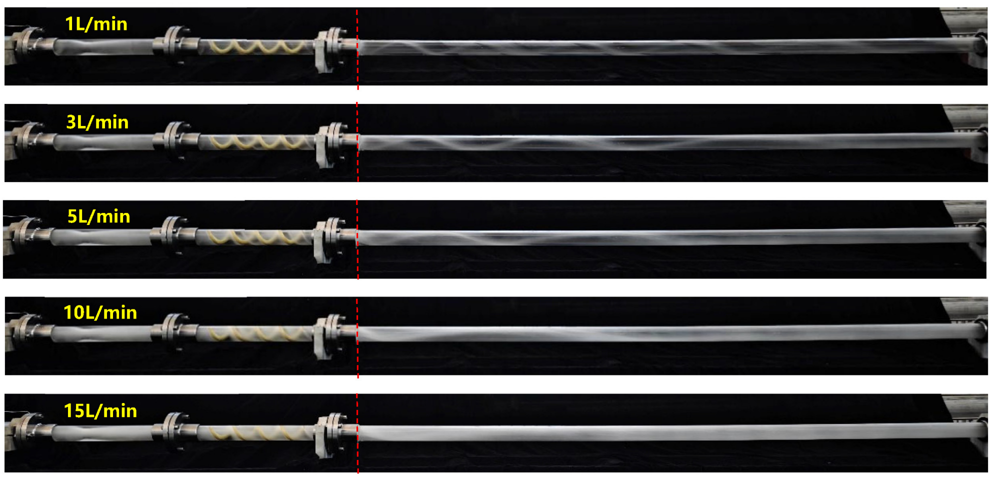

Figure 12. Photographs of spiral flow for the venturi and vortex tool with various liquid flow rates (1, 3, 5, 10, 15 L/min) and the gas flow rate of 600 m^3/h.

As can be observed, as the liquid flow rate increased from 1 L/min to 10 L/min, the length of the spiral flow gradually decreased, and the pitch gradually increased. The flow transitions from spiral laminar flow to unstable flow coupling the spiral and turbulent flow. When the liquid flow rate reached 15 L/min, the typical spiral flow could not be observed, and as a result, it reached the critical liquid flow rate for the tool.

4.4. Pressure Drop with Different Liquid Flow Rates

The instantaneous pressure drops in the horizontal tube (P_1–P_2) are shown in Figure 13 when the gas flow rate is 300 m^3/h and the liquid flow rate is 1, 3, 5, 10, 15 L/min. As can be seen, the pressure drop is less than zero. As the liquid flow rate increases the pressure drop increases, and it tends to become unstable. This effect is consistent with the observed phenomenon of the spiral flow. An elevated liquid flow rate results in greater flow resistance. The negative pressure drop of the venturi accelerated vortex tool is also higher than for the other structures, indicating that this structure can form a more stable spiral flow.

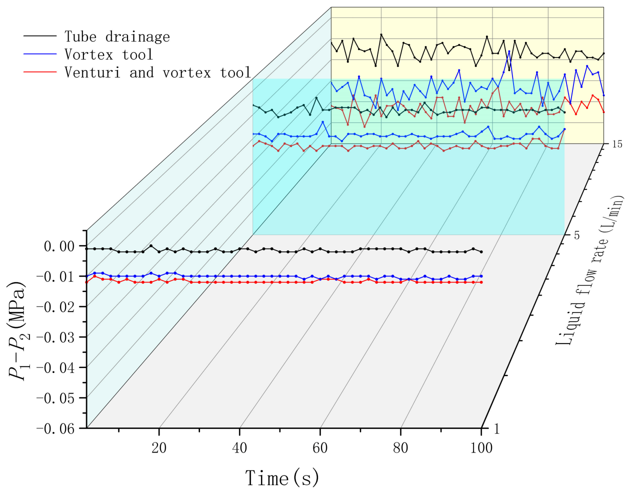

Figure 13. Instantaneous pressure drop of venturi and vortex tool in the horizontal tube with different liquid flow rates (1, 3, 5, 10, 15 L/min) and the gas flow rate of 300 m^3/h. (Supplementary Figure S2).

The average pressure drop in the horizontal tube (P_1–P_2) is shown in Figure 14 for the tube drainage, the vortex tool, and the venturi accelerated vortex tool when the liquid flow rate was 1–15 L/min and the gas flow rate was 300 m^3/h. The average total pressure drop of these (P_1–P_3) is shown in Figure 15.

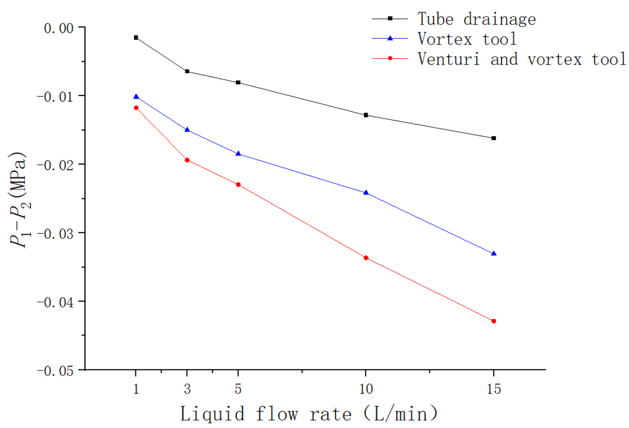

Figure 14. The average pressure drop of different tools in the horizontal tube with different liquid flow rates (1, 3, 5, 10, 15 L/min) and the gas flow rate of 300 m^3/h.

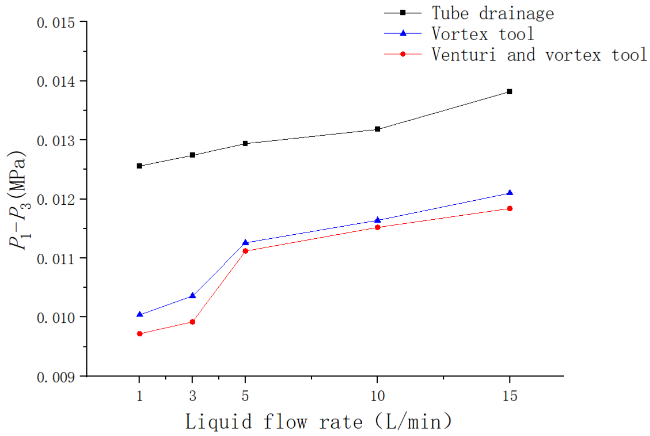

Figure 15. The average total pressure drop of different tools in the horizontal and vertical tube with different liquid flow rates (1, 3, 5, 10, 15 L/min) and the gas flow rate of 300 m^3/h.

As can be ascertained from Figure 14, the average negative pressure drop for the venturi accelerated vortex tool is the highest, followed by the vortex tool, while it is the lowest for the tube drainage. This outcome is consistent with the analysis of spiral flow.

As shown in Figure 15, the average total pressure drop of the horizontal and vertical tubes gradually increases with the increase in liquid flow rate. This effect can be ascribed to the increase in the liquid flow rate that requires greater kinetic energy to carry the liquid out of the tube. Moreover, with the increase in the liquid flow rate, the average total pressure drop of the vortex tool is significantly lower than that of the tube drainage. The overall pressure drop for the venturi accelerated vortex tool is the smallest.

4.5. Performance Analysis of Venturi Accelerated Vortex Tool

To further clarify the performance of the venturi accelerated vortex tool, the results when the liquid flow rate is 1–15 L/min and the gas flow rate is 100–600 m^3/h were also investigated. The lengths of the spiral flow for the venturi accelerated vortex tool with different gas and liquid flow rates are shown in Figure 16. The average horizontal pressure drop and the average horizontal and vertical pressure drop are shown in Figure 17a,b, respectively.

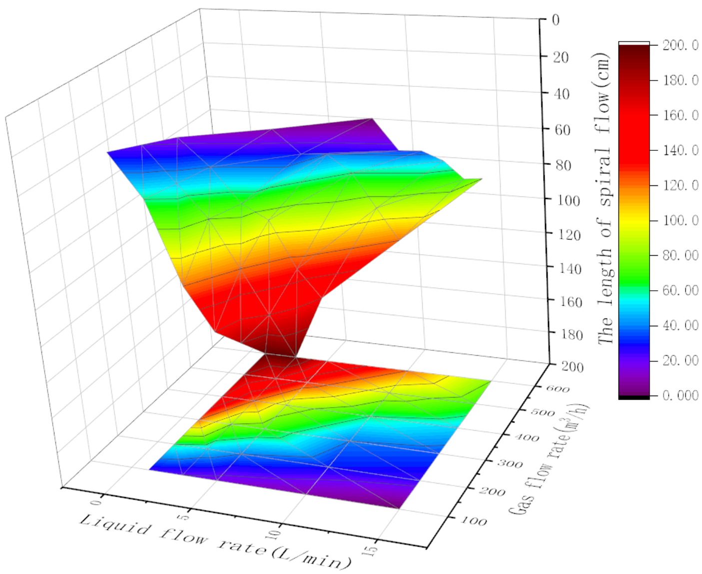

Figure 16. The length of spiral flow for the venturi accelerated vortex tool with liquid flow rate of 1–15 L/min and gas flow rates of 100–600 m^3/h.

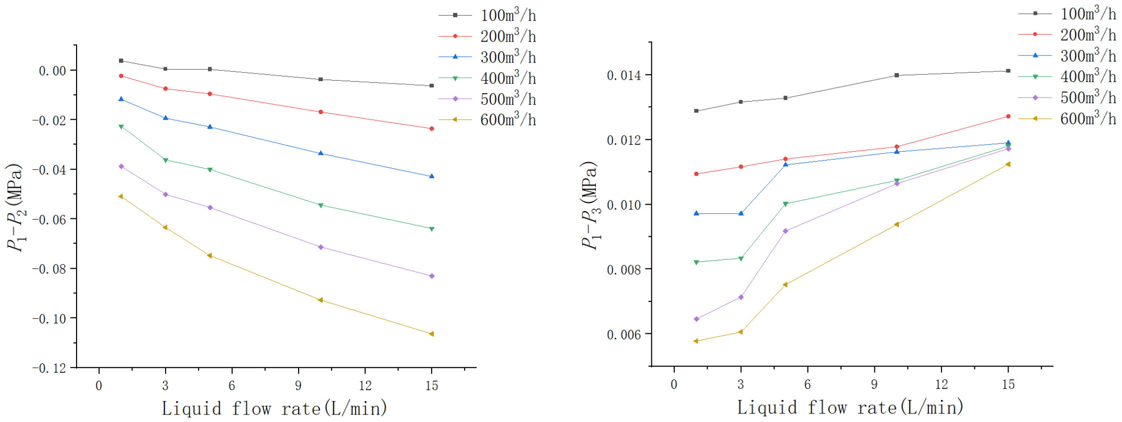

(**a**) The horizontal pressure drop (**b**) The horizontal and vertical pressure drop

Figure 17. The average pressure drop for the venturi accelerated vortex tool with liquid flow rate of 1–15 L/min and gas flow rates of 100–600 m^3/h.

Figure 16 shows that with the decrease in the liquid flow rate and the increase in the gas flow rate, the length of the spiral flow gradually increases. This result can provide guidance for determining the liquid-carrying applicability of the tool under different production conditions. As shown in Figure 17, with the increase in the gas and liquid flow rates, the vacuum degree in the horizontal tube increases, and the total pressure drop in the horizontal and vertical tube increases. Similar results have also been reported by Ali [24], suggesting that the vortex tool was able to reduce the wellbore pressure drop and enhance the production in gas wells. Zhao [18] argued that under the action of vortex downhole tools, the friction factor of the gas–liquid two-phase flow is reduced, as well as the total flow pressure drop. When the gas flow rate was 600 m^3/h and the liquid flow rate increased from 1 L/min to 15 L/min, the vacuum degree in the horizontal pipe increased more than 2 times, while the total pressure drop in the horizontal and vertical pipes increased less than 2 times. In the case of a low liquid flow rate (3 L/min), when the gas flow rate increased from 100 m^3/h to 600 m^3/h, the overall flow resistance loss rapidly decreased by about 54%. These outcomes are in direct line with the analysis results of spiral flow length. Therefore, it can be argued that a longer spiral flow leads to a better spiral laminar flow, which reduces the flow resistance loss.

5. Conclusions

(1) The vortex tool can effectively perform gas–liquid separation in the horizontal tube. This effect is achieved by transforming the turbulent gas–liquid mixture into laminar spiral flow of the liquid near the wall and the gas in the center of the tube. The venturi accelerated vortex tool can significantly improve drainage efficiency, resulting in a longer and more stable spiral flow.

(2) The venturi accelerated vortex tool produced the highest negative pressure in the horizontal tube, followed by the vortex tool alone, and the negative pressure of the tube drainage was the smallest. When the venturi accelerated vortex tool was adopted, only half of the gas flow rate was needed to generate the same negative pressure. This effect was caused by a strong spiral flow, which, in turn, results in the decrease in the total pressure drop in the horizontal and vertical tube.

(3) The increase in the gas flow rate leads to the increase in the length of the spiral flow. As a result, the liquid-carrying capacity is enhanced and the negative pressure in the horizontal tube is exponentially increased. These effects yield a reduction in the total pressure drop in the horizontal and vertical tubes. Especially the venturi accelerated vortex tool exhibits better liquid-carrying performance under these conditions. Under the utilization of a suitable gas flow rate, the length of the spiral flow produced by the venturi vortex tool was longer by about 20% with respect to that formed by the

vortex tool. Its length of the spiral flow and pressure drop with different gas and liquid flow rates was derived, which can provide valuable insights for determining the liquid-carrying applicability of the tool under different production conditions.

(4) When the liquid flow rate increased, the intensity of the spiral flow was initially raised. Subsequently, the unstable flow coupling of spiral and turbulent flows occurs, and the instability of the pressure fluctuations is enhanced. The total pressure drop across the horizontal and vertical tubes also increased. Despite these changes, the drainage performance of the venturi accelerated vortex tool remained superior to that of the vortex tool and the tube drainage.

Supplementary Materials: The following supporting information can be downloaded at: https://www.mdpi.com/article/10.3390/app14072944/s1, Figure S1: Instantaneous pressure drop of different tools in the horizontal tube with liquid flow rate of 3 L/min and gas flow rates of 100–600 m^3/h; Figure S2: Instantaneous pressure drop of venturi and vortex tool in the horizontal tube with different liquid flow rates (1, 3, 5, 10, 15 L/min) and the gas flow rate of 300 m^3/h.

Author Contributions: Conceptualization, overall planning, investigation, H.Z.; methodology, formal analysis, writing—original draft preparation, Y.X.; writing—review and editing, M.C. and J.L.; validation, data curation, M.F.; visualization, X.Z. All authors have read and agreed to the published version of the manuscript.

Funding: This research was funded by National Natural Science Foundation of China (Grant No. 11402051), Natural Science Foundation of Heilongjiang (Grant No. LH2022A004), Natural Science Foundation of Heilongjiang (Grant No. LH2022E016).

Institutional Review Board Statement: Not applicable.

Informed Consent Statement: Not applicable.

Data Availability Statement: The data presented in this study are available on request from the corresponding author.

Conflicts of Interest: The authors declare no conflicts of interest.

References

1. Wang, C.; Dong, B.; Sun, Y.; Du, Q.; Chu, H.; Yi, J. Numerical simulation research of the influencing factor of vortex tool drainage gas recovery technology. *Open Pet. Eng. J.* **2015**, *8*, 64–71. [CrossRef]
2. Guo, T.; Fu, C.; Huang, B.; Zhu, T.; Li, Q.; Yang, H.; Guo, W. Drainage effect of internal vortex tool based on experiment and numerical simulation. *Energy Sources Part A Recovery Util. Environ. Eff.* **2021**. [CrossRef]
3. Gou, R.; Kang, C.; Luo, X. Numerical analysis study on the application of three-lobed vortex tube in low-production wells. *J. Mech. Sci. Technol.* **2023**, *37*, 2969–2980. [CrossRef]
4. Cai, M.; Ma, W.H.; Ma, P.G.; Wang, J.Q.; Li, J.L.; Li, N.; Zhang, H.T. Optimization design and application of vortex drainage gas recovery. In Proceedings of the International Field Exploration and Development Conference 2018 (IFEDC 2018), Xi'an, China, 18–20 September 2018; Springer Series in Geomechanics and Geoengineering. Springer: Singapore, 2020; pp. 1453–1462.
5. Wu, X.; Zhou, C.; An, Y.; Liu, X.; Cen, X. Dynamic analysis of a liquid droplet and optimization of helical angles for vortex drainage gas recovery. *Nat. Gas Ind. B* **2016**, *3*, 339–345. [CrossRef]
6. Zhou, C.; Zhang, T.; Wu, X.; Zhao, F.; Xiong, X. Modeling Study of Wellbore Vortex Flow and Helical Angle Design of Downhole Vortex Tool. In Proceedings of the International Petroleum Technology Conference, Beijing, China, 26–28 March 2019.
7. Zhang, Z.; Liao, R.; Liu, J. Dynamics and effective distance of gas-liquid two-phase swirling flow induced by vortex tools. *Adv. Mech. Eng.* **2018**, *10*, 1–11. [CrossRef]
8. Zhou, C.; Wu, X.; Zhang, T.; Zhao, X.; Gai, S.; Xiang, H. Dynamic analysis for two-phase vortex flow and optimization of vortex tools to unload liquid from gas wells. *J. Pet. Sci. Eng.* **2019**, *173*, 965–974. [CrossRef]
9. Ren, L.; Tang, D.; Zhao, J.; Li, M.; Gan, W. Optimizing the structural parameters of downhole vortex tool in gas well using a genetic algorithm. *J. Pet. Sci. Eng.* **2021**, *200*, 108357. [CrossRef]
10. Guo, H.; Zhou, C.; Jiang, Z.; Zhou, X. Study on separation characteristics of two-phase flow in double helical separator. *Vibroeng. Procedia* **2018**, *19*, 274–278. [CrossRef]
11. Zhang, Z.; Liao, R.; Cai, Z.; Liu, J. An orthogonal numerical simulation experiment study towards the decay characteristics and effective swirl length of the swirling flow in a vortex tool inserted tube. *J. Nat. Gas Sci. Eng.* **2020**, *76*, 103220. [CrossRef]
12. Huang, B.; Li, X.; Fu, C.; Wang, Y.; Cheng, H. The mechanism of drainage gas recovery and structure optimization of an internal vortex tool in a horizontal well. *J. Nat. Gas Sci. Eng.* **2019**, *67*, 233–241. [CrossRef]

13. Zhang, Z.; Liao, R.; Fu, P.; Su, Y.; Luo, W.; Zhang, D. Critical gas velocity prediction for vortex drainage gas wells. *Int. J. Heat Technol.* **2018**, *36*, 1456–1462.
14. Zhang, Z.; Liu, J.; Liao, R.; Cheng, F. Experimental study of swirling flow pneumatic liquid-carrying characteristics in the vortex tool inserted tube under liquid loading conditions. *Exp. Therm. Fluid Sci.* **2023**, *147*, 110954. [CrossRef]
15. Liu, Y.; Xie, C.; Li, X.; Lu, G.; Tang, L.; Tan, X. Optimization analysis of structure parameters of downhole vortex tool based on CFD and orthogonal studies. *J. Pet. Sci. Eng.* **2020**, *190*, 107030. [CrossRef]
16. Lan, W.; Wang, H.; Li, Y.; Feng, K.; Zhang, X.; Liu, Y.; Zhu, X.; Chen, S. Numerical and experimental investigation on a downhole gas-liquid separator for natural gas hydrate exploitation. *J. Pet. Sci. Eng.* **2022**, *208*, 109743. [CrossRef]
17. Han, W.; Li, X.; Su, Y.; Su, M.; Li, R.; Zhao, Y. Effect of Thickness Ratio Coefficient on the Mixture Transportation Characteristics of Helical-Axial Multiphase Pumps. *Appl. Sci.* **2020**, *10*, 345. [CrossRef]
18. Zhang, Z.; Liao, R.; Liu, J.; Ma, J. Mechanism Study and Geometric Parameter Optimization of the Vortex Downhole Tool. *Int. J. Fluid Mach. Syst.* **2019**, *12*, 332–344. [CrossRef]
19. Pakhomov, M.A.; Terekhov, V.I. Eulerian-Eulerian Modeling of the Features of Mean and Fluctuational Flow Structure and Dispersed Phase Motion in Axisymmetric Round Two-Phase Jets. *Mathematics* **2023**, *11*, 2533. [CrossRef]
20. Liang, H.; Miao, W.; Huang, C.; Zhao, B.; Song, H. Gas-liquid two-phase flow characteristics of the jet vortex drainage gas production tool based on computational fluid dynamics. *Asia-Pac. J. Chem. Eng.* **2020**, *15*, e2455. [CrossRef]
21. Liang, H.; Jiang, X.; Li, C.; Ma, J.; Mu, L.; Han, W. Performance study of self-excited oscillatory cyclone drainage tool to improve the efficiency of natural gas well drainage and gas recovery. *Asia-Pac. J. Chem. Eng.* **2023**, *18*, e2912. [CrossRef]
22. Shi, C.; Luo, D.; Zhu, X. Research on the geometry performance of a double-vortex coiled tubing friction-reducing tool based on the Coanda effect. *Geoenergy Sci. Eng.* **2023**, *224*, 211533. [CrossRef]
23. Liu, L.; Liu, J.; He, Z.; Liu, H.; Zhou, C.; Yan, X.; Sun, X. Multi-Objective Optimization of Structural Parameters for Rotary Flow Jetting Tool Based on Orthogonal Experiment. *Int. J. Des. Nat. Ecodyn.* **2020**, *15*, 865–871. [CrossRef]
24. Ali, A.J. Investigation of Flow Modifying Tools for the Continuous Unloading of Wet-Gas Wells. Ph.D. Thesis, Texas A&M University, College Station, TX, USA, 2003.